Cellulose (2018) 25:7189–7196
https://doi.org/10.1007/s10570-018-2073-z

ORIGINAL PAPER

Bacterial cellulose derived monolithic titania aerogel consisting of 3D reticulate titania nanofibers

Bo-xing Zhang · Han Yu · Yubei Zhang · Zhenhua Luo · Weijian Han · Wenfeng Qiu · Tong Zhao

Received: 3 April 2018 / Accepted: 2 October 2018 / Published online: 12 October 2018

Abstract Monolithic titania (TiO_2) aerogel was fabricated by using bacterial cellulose (BC) as the bio-template and preceramic polymer as titanium resource, via freeze-drying and two-step calcination process. As-prepared TiO_2 aerogel BCTi-air-2 h possessed low bulk density (0.04 g/cm^3) and moderate mechanical strength. SEM images showed that TiO_2 aerogel was composed of 3D reticulate TiO_2 nanofibers. The anatase crystalline structure of TiO_2 with crystal size around several nanometers was revealed by XRD measurements. N_2 adsorption/desorption analysis indicated that TiO_2 aerogel possessed high specific area (115 m^2/g) and macroporous structure, which contributed to the high photocatalytic activity. Most importantly, the monolithic state will ease the usage, recycling, and regeneration of TiO_2 aerogel as photocatalyst.

B. Zhang · W. Qiu (✉)
South China Advanced Institute for Soft Matter Science and Technology (AISMST), South China University of Technology (SCUT), 381 Wushan Road, Tianhe District, Guangzhou 510640, China
e-mail: wfqiu@scut.edu.cn

H. Yu · Y. Zhang · Z. Luo · W. Han · T. Zhao (✉)
Laboratory of Advanced Polymer Materials, Institute of Chemistry, Chinese Academy of Sciences, Zhongguancun North First Street 2, Beijing 100190, China
e-mail: tzhao@iccas.ac.cn

Graphical abstract

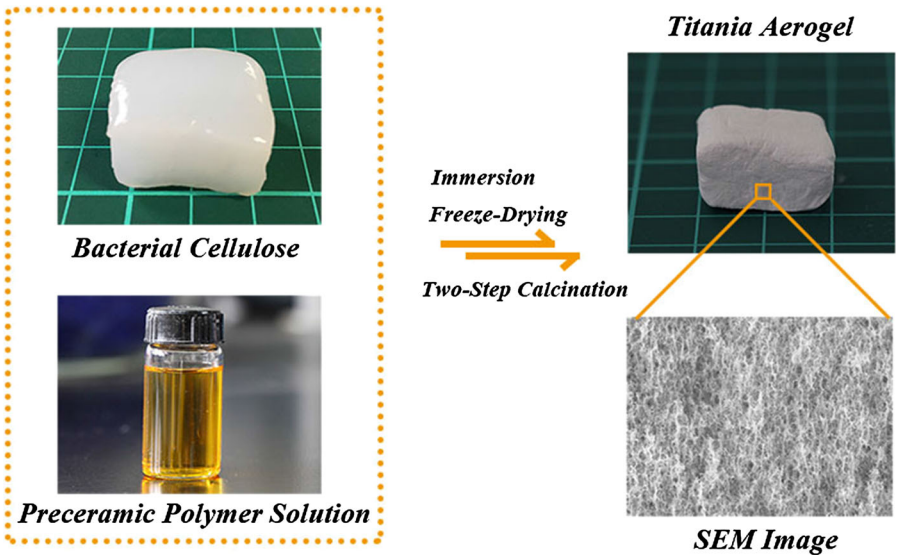

Keywords Titania aerogel · Bacterial cellulose · Preceramic polymer · Bio-template · Photocatalyst

Introduction

In recent decades, bacterial cellulose (BC) attracts more and more attentions not only because of ever-increasing environmental concerns but also because of its unique structure and properties (Foresti et al. 2017; Chen et al. 2013; Lin et al. 2017; Wu et al. 2013). It is an extracellular product of bacteria (normally *Acetobacter xylinum*), possessing excellent mechanical strength, large specific surface area (SSA), and three-dimensional (3D) interconnected porous structure (Svensson et al. 2005; Wu and Cheng 2017; Hsieh et al. 2008). In the catalyst area, BC can be used as an ideal template or catalyst support, because it can simultaneously provide fast mass transfer ability and large space for chemical reactions. In addition, its monolithic state will ease the usage, recycling, and regeneration of catalyst.

Titania (TiO_2) as photocatalyst has been extensively studied, owing to the exceptional performance on wastewater treatment and degradation of volatile organic compounds (VOC) (Liu et al. 2010). Photocatalytic activity of TiO_2 is expected to be effectively enhanced by taking advantage of unique structure of BC. Previously, Zhang and Qi (2005) used BC as a sacrificial template to prepare mesoporous TiO_2 networks consisting of anatase nanowires, but fine structure of BC was destroyed during fabrication process. Dal'Acqua et al. (2015) prepared Au/TiO_2/BC composites by directly mixing TiO_2/Au nanoparticles and BC, but 3D interconnected porous structure of BC also collapsed. Shi et al. (2016) and Liu et al. (2017) fabricated mesoporous SiO_2/$(WO_3)_x$/TiO_2/BC composite aerogels by using small-molecule precursors of TiO_2 as starting materials, combined with the solvothermal method in the presence of BC. Although these composite aerogels retained fine microstructure of BC, carbohydrate nature of BC makes composite aerogels vulnerable under the harsh environments, such as high temperature, humidity, UV light, and acid/base conditions, resulting in poor durability and performance. Moreover, the complete and uniform coating of TiO_2 on the surface of cellulose fibers was difficult to achieve because of poor film-forming properties of TiO_2 nanoparticles and small-molecule precursors of TiO_2 (Luo and Huang 2015). After removal of BC by calcination, monolithic material could not be obtained due to the collapse and shrinkage of 3D interconnected porous structure.

To solve the above problem, preceramic polymers instead of TiO_2 nanoparticles and small-molecule precursors can be used. They possess precise composition and excellent processability. Through curing

and calcination, they can be converted to various types of ceramics such as SiO_2, SiC, SiCO, Si_3N_4, ZrO_2, TiO_2, HfC, TaC, ZrC/SiC, and HfB_2/HfC/SiC/C composite ceramics (Colombo et al. 2010; Cai et al.2013a, b; Lu et al. 2015; Yu et al. 2017). In our previous work, a thin layer of N-doped TiO_2 catalyst was successfully coated on the surface of quartz fabrics by the preceramic polymer route (Yu et al. 2017). In light of excellent film-forming properties of preceramic polymers, complete and uniform coating is possible to form on the surface of cellulose fibers and transform to corresponding ceramic nanofibers through calcination, eventually leading to the prefect replication of fine structure of BC.

Herein, this study aims at fabricating the monolithic TiO_2 aerogel with the well-preserved 3D interconnected porous structure of BC, by using BC as the biotemplate and preceramic polymer as the starting material. A novel fabrication route was developed, and corresponding mechanism was interpreted. The bulk density, morphology, crystalline structure, pore diameter distribution, SSA, and photocatalytic activity of samples were systematically investigated.

Experimental section

Materials

Purified BC sheets with a thickness of 1.5 cm biosynthesized by *Acetobacter xylinum* were kindly offered by Ms C.Y. Zhong (Hainan Yeguo Foods Co., Ltd., Haikou, China). Preceramic polymer aqueous solution (solid content $\approx$ 16 wt%, titanium content $\approx$ 9.4 wt%) was obtained from Tunable Materials Co., Ltd., Suzhou, China. Synthesis of preceramic polymer was described elsewhere in detail (Li et al. 2017). The above raw materials and other reagents were used as received without further treatment.

Preparation of monolithic composite aerogel

First, BC hydrogel was immersed into 0.03 g/mL (concocted according to the solid content) of preceramic polymer solution, and then kept for 48 h to ensure that preceramic polymer was homogeneously dispersed into BC hydrogel. Afterwards, the hydrogel containing preceramic polymer (BCTi hydrogel) was transferred to a plastic container and frozen in liquid N_2 for 15 min, followed by freeze-drying process for 48 h and curing at 200 °C for 2 h. As-obtained sample (BCTi-cured) was kept in a desiccator to avoid adsorption of moisture.

Preparation of monolithic TiO_2 aerogel

To fabricate monolithic TiO_2 aerogel, two steps of calcination process were employed. First, the monolithic composite aerogel BC-cured was heated in a tube furnace under argon (Ar) atmosphere with a programmed temperature (RT $\rightarrow$ 300 °C/1 h $\rightarrow$ 450 °C/2 h with a heating rate of 1 °C/min). As-obtained sample was referred to as BCTi-Ar. Second, BCTi-Ar was calcined again in the tube furnace under air atmosphere with a programmed temperature (RT $\rightarrow$ 450 °C with a heating rate of 1 °C/min). According to different dwelling time at 450 °C, the prepared samples were referred to as BCTi-air-1 h, BCTi-air-2 h, BCTi-air-3 h, respectively.

Photocatalytic activity investigation

Photocatalytic activity of TiO_2 aerogel for degradation of methyl orange was tested under UV light illumination. TiO_2 aerogel (30 mg) was put into a quartz cuvette fulfilled with a 30 mL of methyl orange aqueous solution (15 mg/L). The cuvette was placed in the dark for 30 min to ensure the complete adsorption of methyl orange, and then illuminated by a mercury lamp (500 W). The degradation of methyl orange was monitored by UV–vis spectra (Shimadzu-UV-2600 spectrophotometer).

Characterization and instruments

Freeze-drying procedure was operated on a freeze dryer (LGJ-10E, Four-Ring Science Instrument Plant Beijing Co., Ltd., Beijing, China). Scanning electron microscope (SEM, HITACHI SU8020, Hitachi, Ltd., Tokyo, Japan) was used to observe the morphology of samples. X-ray diffraction (XRD) measurements were performed on a powder diffractometer (Rigaku D/MAX 2500, Rigaku Co., Tokyo, Japan) using a Cu/Ka radiation (40 kV, 200 mA, λ = 1.54056 Å). The specimens were continuously scanned from 3° to 90° (2θ) at a speed of 8°/min. N_2 adsorption/desorption isotherms were measured at 77 K on a surface area and porosity analyzer (Micromeritics ASAP

2020, Micromeritics Instrument Co., Norcross, GA, USA).

Results and discussion

Route and mechanism for fabrication of monolithic TiO_2 aerogel

When preceramic polymer was directly treated by freeze-drying, samples severely cracked. After the introduction of BC, composite aerogel with intact shape can be obtained by freeze-drying, suggesting that BC had a strengthening effect on preceramic polymer matrix. However, TiO_2 aerogel still easily cracked when composite aerogel was simply calcined in air. Through many efforts, monolithic TiO_2 aerogel with intact shape was successfully prepared by an optimized route as shown in Fig. 1.

In the first step, preceramic polymer aqueous solution with the suitable concentration (around 0.03 g/mL) need to be prepared, because higher concentration will result in coalescence of microstructure, while lower concentration will cause dramatic shrinkage. Then, BC hydrogel was immersed into this solution and held for 48 h to ensure the homogeneous dispersion of preceramic polymer in the hydrogel. Ice crystals were generated and gradually grew during freezing in liquid N_2. Meanwhile, preceramic polymer was precipitated from the solution and expelled to the boundary between cellulose fibers and ice crystals, leading to the formation of a thin layer of coating on the surface of cellulose fibers. After freezing procedure, 3D reticulate cellulose nanofibers coated with preceramic polymers would exist in ice crystals like impurity. Subsequently, ice crystals were removed by sublimation in freeze-drying process to avoid the collapse of fine structure of pristine BC, leaving preceramic polymer to attach to the surface of cellulose nanofibers. After curing at 200 °C preceramic polymer was fixed on the surface of cellulose nanofibers through chemical reactions between preceramic polymer and hydroxyl groups of cellulose fibers. The bulk density (Table 1) of yellow BCTi-cured aerogel (Fig. 2) was 0.03 g/cm^3, obviously higher than that (0.01 g/cm^3) of BC aerogel due to the incorporation of preceramic polymer.

To get monolithic TiO_2 aerogel, two-step calcination process was employed. In the first calcination process, Ar was used as protecting and carrier gas, and composite aerogel was carbonized at 450 °C for 2 h to form the core–shell structure (Fig. 1). The inner layer was composed of carbon nanofibers which derived from the carbonization of cellulose nanofibers (Wu et al. 2013). The outer layer was composed of coating of TiO_2 nanoparticles and free carbon which came from carbonization of preceramic polymer. Carbon nanofibers will enhance the strength of aerogel and aid

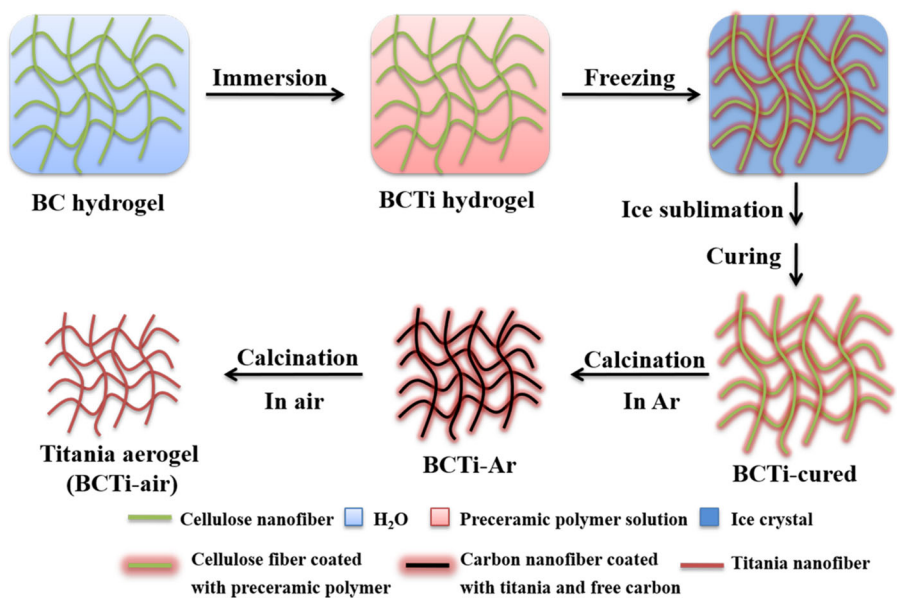

Fig. 1 The route and mechanism for fabrication of monolithic TiO_2 aerogel

Table 1 Properties of BC and BCTi samples

	Linear shrinkage[a] (%)	Density (g/cm^3)	BET surface area (m^2/g)	Pore volume (cm^3/g)	Crystallinity[b] (%)
BC	< 1	0.010	102	0.39	–
BCTi-cured	< 1	0.030	291	0.20	25.0
BCTi-Ar	11	0.033	267	0.26	28.8
BCTi-air-1 h	19	0.040	152	0.21	68.3
BCTi-air-2 h	22	0.045	115	0.17	69.0
BCTi-air-3 h	24	0.047	102	0.16	74.6

[a]The shrinkage of BC and BCTi samples in the length direction was calculated corresponding to BC hydrogel and BCTi hydrogel, respectively

[b]Crystallinity was calculated using the software (Xpert Highscores ver3.0)

Fig. 2 Photos of BC and BCTi samples. The size of one grid in the background plate is 1 cm × 1 cm

the maintaining of 3D reticulate structure. Without the strengthening and supporting effects of carbon nanofibers, the decomposition of BC and preceramic polymer during calcination process will result in collapse and crack of aerogel. This explained why monolithic TiO_2 aerogel could not be obtained by the direct calcination in air. After the first calcination, most of shrinkage had occurred, and the shrinkage in the second calcination process will be alleviated. During the second calcination process, residual carbon was gradually removed. At the same time, TiO_2 nanoparticles were sintered and connected with each other to endow monolithic TiO_2 aerogel with moderate mechanical strength for handling.

Finally, through immersion, freeze-drying, two-step calcination process, the pure monolithic TiO_2 aerogel BCTi-air (Fig. 2) with a low bulk density of 0.04 g/cm^3 and moderate mechanical strength was successfully fabricated.

Morphology observation

The homogeneous 3D interconnected porous structure of BC aerogel was observed in SEM images (Fig. 3). Through freeze-drying and curing procedures, the complete and uniform coating on the surface of cellulose nanofibers was shown, due to the excellent film-forming properties of preceramic polymers. After treatment at 450 °C for 2 h in Ar, 3D interconnected porous structure was well preserved, attributed to the strengthening and supporting effects of carbon nanofibers in BCTi-Ar. After the second calcination, fine structure of BC still remained in BCTi-air-1 h, BCTi-air-2 h, and BCTi-air-3 h. Based on these observations, it was confirmed that TiO_2 aerogel had perfectly replicated the unique structure of BC.

Crystalline structure evolution

Main characteristic peaks of BC were shown at 2θ = 14.8°, 16.3°, and 22.7° (Fig. 4), which were assigned to cellulose I structure (Zhang et al. 2015). After curing at 200 °C, the wide peaks belonging to anatase phase (PDF card no. 73-1764) appeared, indicating that TiO_2 crystals was generated. In BCTi-Ar, similar peaks were displayed, revealing that crystal size was kept unchanged. The residual carbon derived from the first calcination process may function as impurity to inhibit growth of TiO_2 crystals. Once residual carbon was removed, characteristic peaks of anatase phase in BCTi-air-1 h became sharper, indicating growth of TiO_2 crystals. With increase of

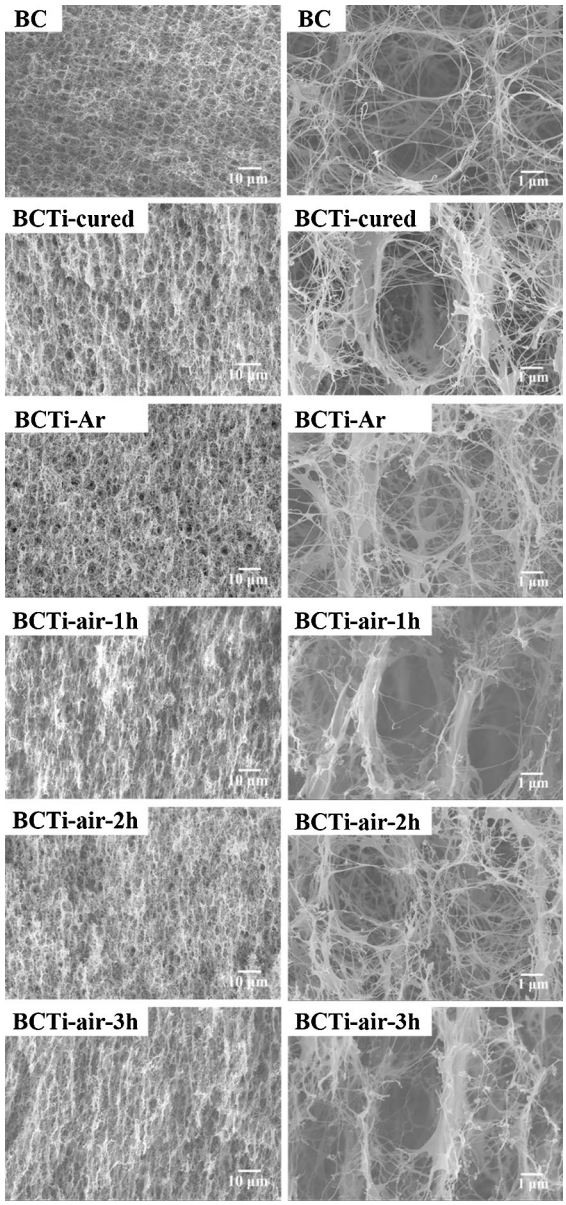

Fig. 3 SEM images of BC and BCTi samples

dwelling time at 450 °C, TiO_2 crystals further grew, as suggested by the intensified XRD signals. For BCTi-air-2 h, the crystal size was calculated as 6.8 nm according to the Scherrer equation. As aforementioned, all of BCTi-air aerogels possessed typical crystalline structure of TiO_2 with anatase as the single phase.

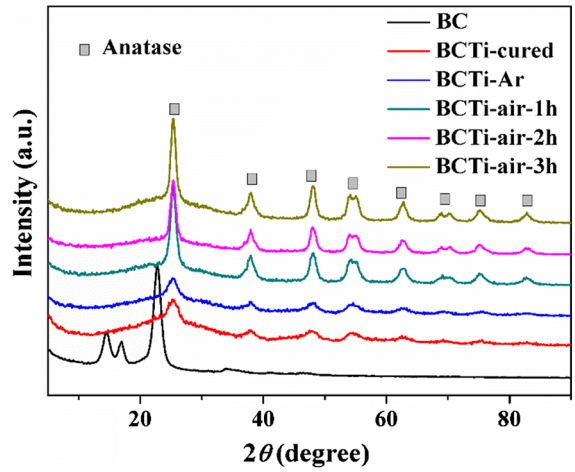

Fig. 4 XRD patterns of BC and BCTi samples

N_2 adsorption/desorption analysis

N_2 adsorption/desorption results of BC, and BCTi samples were shown in Fig. 5 and Table 1. BC displayed type II isotherms, indicating the existence of macropores which can be also observed in SEM images (Fig. 3). 3D reticulate nanofibrous structure were responsible for the large SSA (102 m^2/g) of BC. After incorporation of preceramic polymer, SSA of BCTi-cured was greatly increased to 291 m^2/g which was higher than that (220 m^2/g) of previous reports (Foresti et al. 2017), because preceramic polymer coating would provide much more fine structure. A slight decrease was shown for BCTi-Ar, caused by pyrolysis of preceramic polymer. After removal of residual carbon, SSA was dramatically decreased to 115 m^2/g, which was higher than that (61 m^2/g) of reported pure TiO_2 aerogel derived from BC template (Zhang and Qi 2005), mainly because of the disappearance of fine structure derived from residual carbon. Moreover, with the increase of dwelling time at 450 °C, SSA was further decreased because of the shrinkage of skeleton and the growth of TiO_2 crystals. N_2 adsorption/desorption analysis revealed that monolithic TiO_2 aerogel possessed 3D interconnected macroporous structure and large SSA. The former will give TiO_2 aerogel with fast mass transfer ability, and the latter will provide large space for chemical reactions.

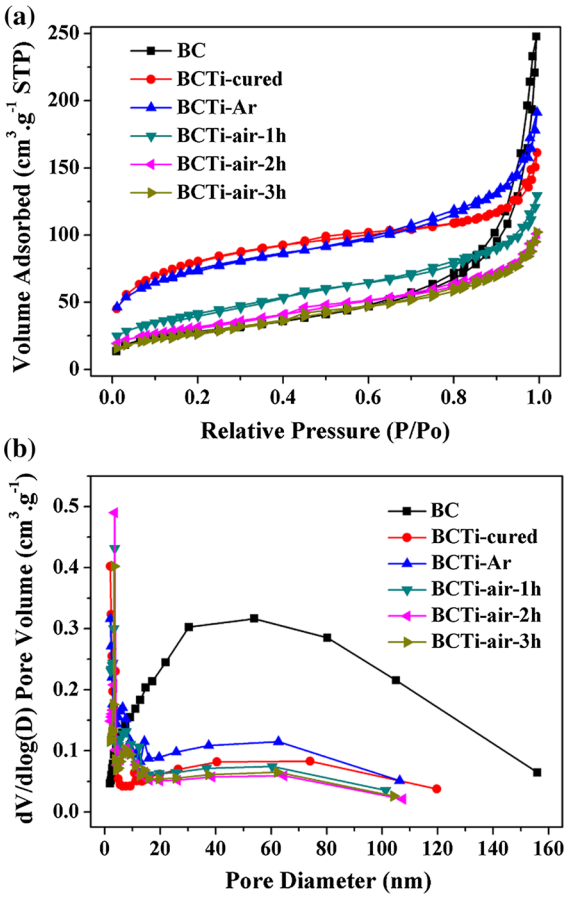

Fig. 5 **a** N_2 adsorption/desorption isotherms and **b** pore diameter distribution of BC and BCTi samples

Photocatalytic activity study

Photocatalytic degradation of methyl orange under UV light was performed to evaluate photocatalytic activity of TiO_2 aerogel. For BCTi-air-1 h, BCTi-air-2 h, and BCTi-air-3 h, most of methyl orange was degraded within 12 min (Fig. 6). Among them, BCTi-air-2 h demonstrated the highest photocatalytic activity. In the case of BCTi-1 h-air, although SSA was the highest, trace amount of residual carbon may exist, deteriorating photocatalytic activity of TiO_2 crystals (Fig. 4). Whereas, for BCTi-air-3 h, the inferior photocatalytic activity was caused by decrease of SSA. Although the monolithic TiO_2 aerogel demonstrated a little lower photocatalytic efficiency compared to nanopowder P25 (commercial TiO_2 nanopowder, commonly used as the benchmark), in contrast, the monolithic state of TiO_2 aerogel will facilitate separation and regeneration, and eventually ease practical applications.

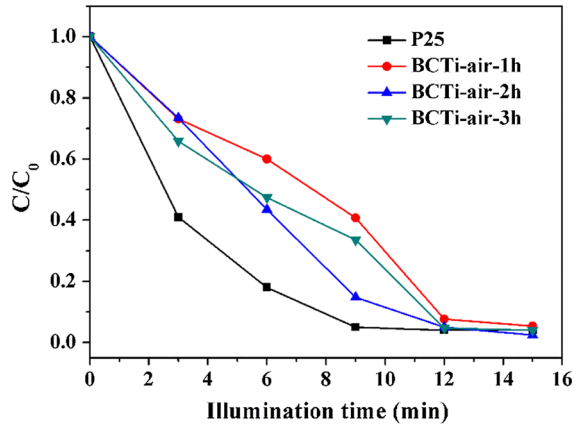

Fig. 6 Variations of the concentration of methylene orange in aqueous solution as a function of illumination time

Conclusions

In this work, monolithic TiO_2 aerogel was successfully fabricated, by using BC as the bio-template and preceramic polymer as titanium resource, via the freeze-drying and two-step calcination process. As-obtained TiO_2 aerogel possessed 3D reticulate nanofibrous structure, low bulk density, moderate mechanical strength, and high photocatalytic activity under UV light. These merits suggest that it may have great potential applications for photocatalyst. Moreover, the TiO_2 aerogel may serve as a platform, on which sensors, electrode materials, and other catalyst systems can be engineered by doping.

Acknowledgments This work is financially supported by the grants of the China Postdoctoral Science Foundation (No. 2017M612655). The authors also gratefully acknowledge the financial support from the Pearl River Talent Scheme (No. 2016ZT06C322).

References

Cai T, Qiu W, Liu D, Han W, Ye L, Zhao A, Zhao T (2013a) Synthesis of soluble poly-yne polymers containing zirconium and silicon and corresponding conversion to nano-sized ZrC/SiC composite ceramics. Dalton Trans 42:4285–4429

Cai T, Qiu W, Liu D, Han W, Ye L, Zhao A, Zhao T (2013b) Synthesis, characterization, and microstructure of hafnium

boride-based composite ceramics via preceramic method. J Am Ceram Soc 96:1999–2004

Chen L, Huang Z, Liang H, Guan Q, Yu S (2013) Bacterial-cellulose-derived carbon nanofiber@MnO_2 and nitrogen-doped carbon nanofiber electrode materials: an asymmetric supercapacitor with high energy and power density. Adv Mater 25:4746–4752

Colombo P, Mera G, Riedel R, Sorarù GD (2010) Polymer-derived ceramics: 40 years of research and innovation in advanced ceramics. J Am Ceram Soc 93:1805–1837

Dal'Acqua N, Mattos AB, Krindges I, Pereira MB, Barud HS, Ribeiro SJL et al (2015) Characterization and application of nanostructured films containing Au and TiO_2 nanoparticles supported in bacterial cellulose. J Phys Chem C 119:340–349

Foresti ML, Vázquez A, Boury B (2017) Applications of bacterial cellulose as precursor of carbon and composites with metal oxide, metal sulfide and metal nanoparticles: a review of recent advances. Carbohydr Polym 157(Supplement C):447–467

Hsieh YC, Yano H, Nogi M, Eichhorn SJ (2008) An estimation of the Young's modulus of bacterial cellulose filaments. Cellulose 15:507–513

Li Y, Pan X, Yang Z (2017) A method for preparation of the titania precursor and its solution. CN 2017113044355

Lin SP, Kung HN, Tsai YS, Tseng TN, Hsu KD, Cheng KC (2017) Novel dextran modified bacterial cellulose hydrogel accelerating cutaneous wound healing. Cellulose 24:4927–4937

Liu G, Wang L, Yang H, Cheng H, Lu G (2010) Titania-based photocatalysts-crystal growth, doping and heterostructuring. J Mater Chem 20:831–843

Liu D, Shi F, Liu J, Hu S, Yu L, Liu S et al (2017) Synthesis of SiO_2–W_xTiO_2 composite aerogels via solvothermal crystallization under the guidance of bacterial cellulose followed by freeze drying method. J Sol Gel Sci Technol 84:42–50

Lu Y, Ye L, Han W, Sun Y, Qiu W, Zhao T (2015) Synthesis, characterization and microstructure of tantalum carbide-based ceramics by liquid polymeric precursor method. Ceram Int 41:12475–12479

Luo Y, Huang J (2015) Hierarchical-structured anatase-titania/cellulose composite sheet with high photocatalytic performance and antibacterial activity. Chem Eur J 21:2568–2575

Shi F, Yu T, Hu S, Liu J, Yu L, Liu S (2016) Synthesis of highly porous SiO_2–$(WO_3)_x$·TiO_2 composite aerogels using bacterial cellulose as template with solvothermal assisted crystallization. Chem Eng J 292(Supplement C):105–112

Svensson A, Nicklasson E, Harrah T, Panilaitis B, Kaplan DL, Brittberg M et al (2005) Bacterial cellulose as a potential scaffold for tissue engineering of cartilage. Biomaterials 26:419–431

Wu CN, Cheng KC (2017) Strong, thermal-stable, flexible, and transparent films by self-assembled TEMPO-oxidized bacterial cellulose nanofibers. Cellulose 24:269–283

Wu Z, Li C, Liang H, Chen J, Yu S (2013) Ultralight, flexible, and fire-resistant carbon nanofiber aerogels from bacterial cellulose. Angew Chem 125:2997–3001

Yu H, Ye L, Zhang T, Zhou H, Zhao T (2017) Synthesis, characterization and immobilization of N-doped TiO_2 catalysts by a reformed polymeric precursor method. RSC Adv 7:15265–15271

Zhang D, Qi L (2005) Synthesis of mesoporous titania networks consisting of anatase nanowires by templating of bacterial cellulose membranes. Chem Commun 21:2735–2737

Zhang B, Azuma J, Uyama H (2015) Preparation and characterization of a transparent amorphous cellulose film. RSC Adv 5:2900–2907